Field-Experience Based Root-Cause Analysis of Power-Converter Failure in Wind Turbines

Katharina Fischer, Thomas Stalin, Hans Ramberg, Jan Wenske, Göran Wetter, Robert Karlsson, and Torbjörn Thiringer, *Senior Member, IEEE*

***Abstract*—The frequent power-converter failure experienced in wind turbines has a strong economic impact through both the related turbine unavailability and the maintenance cost. Up to now, the prevailing mechanisms and causes underlying the converter failure in wind turbines are mostly unknown. Their identification is, however, a prerequisite for the development of effective solutions. This paper describes a multitrack empirical approach to failure analysis including systematic field-data evaluation, exploration of the real converter operating environment, and postoperational laboratory investigation of converter hardware. The analysis is carried out for two widely used multi-MW wind turbines with low-voltage, insulated-gate bipolar transistor-based converters (topology 1: doubly fed induction generator with partially rated converter, topology 2: induction generator with fully rated converter). The findings suggest that the principle failure mechanisms of power electronics found in other applications, namely solder degradation and bond-wire damage, play a minor role in the investigated types of wind turbines. Instead, the analysis reveals indications of insufficient protection of the converter hardware against the environment (salt, condensation, and insects) as well as indications of electrical overstress.**

***Index Terms*—Converter, failure, power electronics, reliability, root-cause analysis, wind turbine.**

I. Introduction

POWER converters are a frequent source of failure in modern wind turbines. In a reliability field-study on pitch-controlled, variable-speed onshore wind turbines with rated capacity ≥850 kW, in which more than 31 000 downtime events were evaluated, the frequency converters were found to have caused 13% of the failures and 18% of the downtime of the monitored turbines [1]. A similar picture concerning the converter reliability was previously obtained by Spinato *et al.* [2] in a reliability study on an older population of wind turbines, for which data from more than 6000 onshore wind turbines in Denmark and Germany collected through a period of 11 years was evaluated: with an average number of approximately 0.2 failures per turbine and year, around a fifth to a seventh of the overall failure rate of the considered wind turbines was caused by the converter system.

In addition, the reliability-study results are consistent with similar experience made by numerous wind-turbine operators and maintenance service-providers worldwide, where the limited converter reliability is considered a major cost driver. In the increasing number of offshore wind parks, the impact of a high failure rate on turbine downtime is even more severe due to the fact that the accessibility of offshore installations for repair is constrained by wave-height and wind conditions. Apart from the repair cost and revenue loss resulting from turbine downtime, power-converter failure is also afflicted with a risk of substantial secondary damage, as it is a common cause of fire in wind turbines [3]. In summary, it can be stated that the high failure rates of power converters are not a problem being limited to single wind-turbine manufacturers, models or sites, but are a common and important challenge to be solved in order to further reduce the cost of wind energy. However, a crucial prerequisite for the development of remedial measures is to understand the mechanisms and causes underlying the converter failures. This is the subject of the present paper.

A. Power Converters in Wind Turbines

Almost all modern wind turbines have designs allowing variable-speed operation, both for efficiency and load-reduction purposes. The generator-converter topologies commonly used in wind turbines are: 1) an induction generator with a full-scale converter; 2) an either permanent-magnet or electrically excited synchronous generator (PMSG, EESG) with a full-scale converter; and 3) a doubly fed induction generator (DFIG) with a partially rated converter. In all these topologies, the power-electronic converters are required to decouple the rotational speed of the drive-train, i.e., the generator frequency, from the frequency of the electric power grid. A comprehensive overview of the different power-electronic converters used in wind turbines, including low-voltage and medium-voltage topologies, is given in [4]. The largely prevailing type of converter system is a low-voltage, insulated-gate bipolar transistor (IGBT)-based, two-level converter in back-to-back configuration, in which a

Manuscript received March 31, 2014; revised July 30, 2014; accepted August 11, 2014. Date of publication October 7, 2014; date of current version December 23, 2014. This work was supported by the Swedish Research Program Vindforsk III. Recommended for publication by Associate Editor B. Mather.

K. Fischer was with the Division of Electric Power Engineering, Department of Energy and Environment, Chalmers University of Technology SE-412 96 Gothenburg, Sweden. She is now with the Fraunhofer Institute for Wind Energy and Energy System Technology (IWES), D-30167 Hannover, Germany (e-mail: katharina.fischer@iwes.fraunhofer.de).

T. Stalin is with Vattenfall Wind Power, SE-169 56 Stockholm, Sweden (e-mail: Thomas.stalin@vattenfall.com).

H. Ramberg is with Volvo Car Corporation, SE-418 78 Gothenburg, Sweden (e-mail: hans.ramberg@volvocars.com).

J. Wenske is with the Fraunhofer Institute for Wind Energy and Energy System Technology (IWES), D-27572 Bremerhaven, Germany (e-mail: jan.wenske@iwes.fraunhofer.de).

G. Wetter is with Swerea IVF AB, SE-431 53 Gothenburg, Sweden (e-mail: goran.wetter@swerea.se).

R. Karlsson and T. Thiringer are with the Division of Electric Power Engineering, Department of Energy and Environment, Chalmers University of Technology, SE-412 96 Gothenburg, Sweden (e-mail: robert.karlsson@chalmers.se; torbjorn.thiringer@chalmers.se).

Color versions of one or more of the figures in this paper are available online at http://ieeexplore.ieee.org.

Digital Object Identifier 10.1109/TPEL.2014.2361733

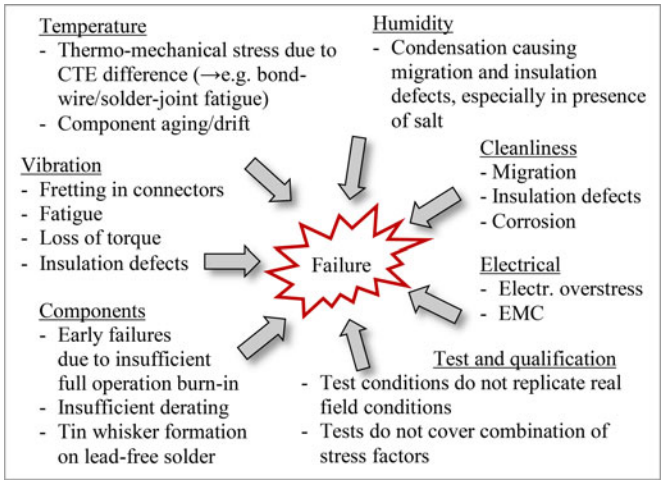

Fig. 1. Common causes of failures in electronics.

generator-side and a grid-side converter are connected through a dc-voltage intermediate link.

There are two different packaging types for power devices: 1) press-pack technology, which is proposed for application in medium-voltage converters in multi-MW wind turbines [5] and is characterized by a high reliability and cost; and 2) module technology, which is the common packaging technology in contemporary wind turbines. Herein, the power-electronic chips (IGBTs, diodes) are electrically contacted by means of bond wires. The chips are soldered to an insulating ceramic substrate, also called direct copper bonded substrate (DCB). There are power modules with and without a base plate. In the first case, the substrate is soldered to a base plate of copper, which in turn is attached to the heat sink by means of thermal grease. In designs without a baseplate, the DCB substrate is directly attached to the heat sink.

B. Failure Mechanisms and Causes

The objective of a failure analysis is to identify the failure mechanisms and to find out the failure causes. As defined in [6], in this context, the mechanism denotes the physical, chemical or other process that leads to a failure. The cause of a failure can be intrinsic, due to weaknesses in the item or wear out, or extrinsic, e.g., due to use outside the design specifications. A general, application-independent overview of common causes of failures in electronics is given in Fig. 1. It shows the wide variety of potential influencing factors and illustrates the complexity of a root-cause analysis. A review of general failure mechanisms in power-electronic converters with a particular focus on packaging-level and chip-level effects is found in [7]–[9]. Industry-survey based results concerning the subassemblies or components in power converter systems that are most frequently giving rise to a failure is provided in [10] and [11].

In the wind-power specific literature dealing with converter reliability, a clear focus is set on the power modules containing the power-electronic devices and on their "classical" principle failure mechanisms as known from other applications [12]–[17]: 1) the lift-off or fatigue-damage of the bond wires, resulting from thermal cycling of adjacent materials with different thermal-expansion coefficients; and 2) the fatigue of die-attach or baseplate solder joints, once again due to thermomechanical stress, which leads to a gradual delamination resulting in overheating and thermal failure. An experimental result of bond-wire damage is shown, e.g., in [18] and delamination at the die backside/solder area is experimentally shown as a function of the number of cycles in [19] and [22]. Thermal modeling procedures of semiconductor components for various applications, see for instance [20], [21], are fairly mature today. Also, experimental verification on the thermal behavior of semiconductors can be found in the literature, e.g., by means of monitoring the module thermal resistance as demonstrated in [22]. Besides the converter reliability-related literature focusing on the power-electronic devices and their packaging, an overview on reliability aspects of dc-link capacitors in power electronic converters is found in [23].

As a consequence of the predominant focus on bond-wire and solder fatigue, the attention in the wind-turbine converter specific literature is directed primarily to the generator-side converters in turbines with DFIG [24]–[28] and with low-speed PMSG [29], [30]. Due to the fact that these are subject to high currents at low frequencies, which causes severe thermal cycling as explained in [31], this is considered to be the most critical converter subsystem with respect to reliability.

Apart from some forensic analysis by Bartram [25] on power modules, which had failed in the field, the previous research on wind-turbine converter reliability described in the literature has primarily used simulation as well as lab experiments under defined stress conditions. In most cases, the objective has been to estimate the reliability or calculate a lifetime consumption under a given "mission profile."

This paper takes the opposite way, which is to the knowledge of the authors a novel approach in the present context: by means of empirical failure analysis based on a systematic evaluation of historical field-data, on directed measurements in the field and on postoperational analysis of converter hardware, this work seeks to identify the prevailing failure mechanisms and causes of the observed frequent converter failure in two different types of wind turbines. In this way, it aims to provide a basis for the development of effective countermeasures as well as for focusing research on the failure mechanisms being most relevant in the field. In a larger context, the present work tackles the "lack of understanding in failure mechanisms and failure modes of reliability critical components," which in [26] has been pointed out as one of today's key challenges in the research on reliability for power electronic systems.

C. Paper Outline

The subsequent parts of the paper are structured as follows: Section II describes the investigated two wind-turbine systems and their power converters. Section III introduces the field-experience based, multitrack approach used in this paper and the details of the applied analysis methods. The analysis results are presented and discussed in Section IV, and conclusions of

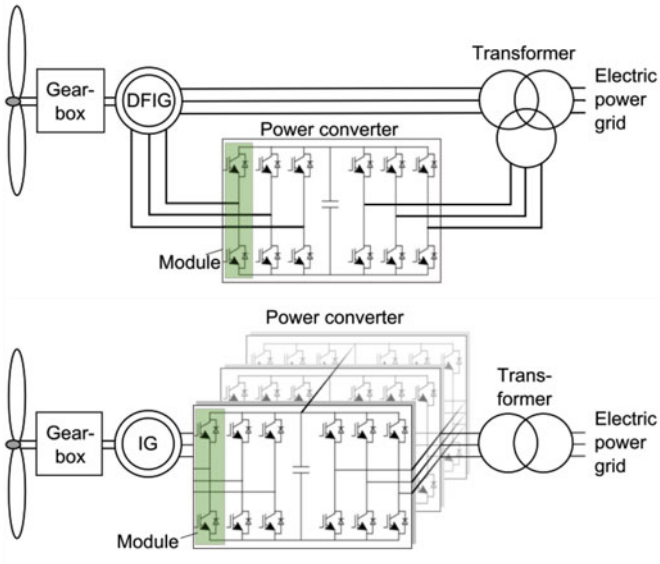

Fig. 2. Generator–converter topologies of wind turbines types WT1 (top) and WT2 (bottom).

TABLE I
PROPERTIES OF THE INVESTIGATED WIND TURBINES WT1 AND WT2 AND THEIR CONVERTER SYSTEMS

	Wind turbine type WT1	Wind turbine type WT2
Drive train	Geared, distributed	
Generator	DFIG	Squirrel-cage IG
Converter location	Inside nacelle	Tower bottom
Converter rating	Partially rated	Fully rated
Converter technology	IGBT based, low-voltage, back-to-back VSC	
Number of power modules	6 (grid-side converter: 3, generator-side conv.: 3)	18 (grid-side conv.: 3×3, gen.-side conv.: 3×3)
Power module details	Water-cooled design without baseplate, integrated gate driver board, identical manufacturer	

the work together with an outlook to ongoing continued research on the topic of reliable power converters for wind turbines are provided in Section V.

II. INVESTIGATED SYSTEMS

The analysis focuses on two wind-turbine types with low-voltage IGBT-based two-level voltage-source converter (VSC) systems. In order to ensure confidentiality, the exact turbine types investigated in this analysis will not be provided and will therefore be referred to as wind turbines WT1 and WT2. The turbines have a similar rated capacity in the range of several megawatts. The following sections give a short description of their generator-converter topologies, which are shown in Fig. 2, and properties relevant for the analysis. A summary of the key properties of the investigated systems is provided in Table I.

A. Wind Turbine WT1

The turbine referred to as WT1 is equipped with a four-pole DFIG with wound rotor. The generator stator feeds the 690 V side of the turbine transformer and is in this way directly coupled to the electric power grid. The partially rated converter controlling the generator rotor current is connected to the 480 V output of the transformer. The converter consists of three modules on the generator side and three modules on the grid side (back-to-back configuration), which are connected through the dc link; see Fig. 2 (top). Each of these modules consists of hard-connected, paralleled half-bridges, which are controlled by a single gate-driver board. The half-bridges in turn consist of a larger number of synchronously switched IGBTs and their respective freewheeling diodes to provide the overall current capacity. The electrical contact between the power-electronic chips and the driver board is provided by means of metallic springs. The power modules have a design without a baseplate, i.e., the DCB substrate is directly attached to the water-cooled heat sink. Fault-ride through capability of the wind turbine is provided by means of choppers connected to the dc link. In the WT1 system, the power converter is located inside the nacelle. Both the generator and the converter are specified to have an ingress protection class of IP54.

B. Wind Turbine WT2

The wind-turbine system referred to as WT2 uses an asynchronous generator with squirrel-cage rotor. As shown in Fig. 2 (bottom), its stator is connected to the 690 V side of the turbine transformer through a full-scale power converter (FPC). Also, the converter system of WT2 has fault ride-through capability.

Both the generator-side and the grid-side converter of WT2 consist of three units, each of which contains three power modules, resulting in a total number of 18 modules. As shown in Fig. 2, the units are hard-connected in parallel both on the ac and the dc side. The current sharing between the paralleled units is monitored by the control system, which stops the turbine when the current unbalance between the units exceeds a predefined threshold value. The water-cooled power modules used in the converter of WT2 are of a similar type as the ones applied in WT1 and come from the same manufacturer. In contrary to turbine WT1, the power-converter system of WT2 is located at the bottom of the turbine tower.

III. METHODS OF ANALYSIS

With the objective to identify the dominant failure modes and causes of converter failure in wind turbines, a multitrack approach is used: it combines comprehensive failure-data analysis, an investigation of the operating environment of the power converters in the field, and a postoperational analysis of converter hardware. The results of these three different tracks, which are explained in more detail in the following, have been evaluated in a multidisciplinary root-cause analysis team. Note that based on prioritization by the wind-turbine operator, the investigation has been concentrated solely on failures of power modules (incl. the integrated gate driver board). Failures of other parts of the converter system like, e.g., the dc-link capacitors, the cooling system or the main control board have not been included in this analysis.

A. Failure-Data Analysis

The failure-data analysis is based on data from one onshore and two offshore wind parks with the turbine types of interest, all of which are located in a radius of 700 km. The parks are operating in similar climatic conditions with respect to temperature and relative humidity, with the only exception of the onshore park being located in a region with lower average temperatures. The failure-data analysis covers in total approximately 170 turbines and 370 operational years. More in detail, the analyzed data comprises:

1) converter (i.e., power-module) failure data, compiled based on maintenance records from the period 2008–2012,
2) SCADA status logs and selected SCADA signals in a temporal resolution of 10 min covering the years 2009 and 2010,
3) climate data: daily average values of the ambient temperature and relative humidity at two offshore sites, daily number of lightning strikes in vicinity to one of these sites, from the periods covered by the failure and SCADA data.

A common measure for assessing the reliability of a component, particularly in lack of information about the component age, is the average failure rate. This is defined as

$$f = \frac{\sum_{i=1}^{I} N_i}{\sum_{i=1}^{I} X_i \cdot T_i} \tag{1}$$

with N_i denoting the number of failures of the component in the time interval *i*, X_i describing the number of systems reporting to the database in time interval *i*, and T_i being the duration of the time interval *i*. All failure rates are given in failures per system and year.

In this study, the average failure rates are analyzed in order to identify potential differences related to the turbine topology or the site being located onshore versus offshore. With the objective to reveal possible age- or season-related changes in the converter reliability, the temporal evolution of the average annual and monthly failure rates is analyzed. For two large offshore wind parks with turbines of type WT1 and WT2, respectively, the available failure data have been analyzed together with climate data in order to identify to which extent the environmental conditions ambient temperature, ambient relative humidity, wind speed and lightning strikes are correlated with converter failure.

For this purpose, a simple linear correlation analysis is carried out: The linear (also: Pearson's) correlation coefficient quantifies the strength of a linear relationship between two variables *X* and *Y*. From a series of *n* measured pairs of *X* and *Y*, denoted x_i and y_i, the linear correlation coefficient of the population is estimated using

$$r_{xy} = \frac{\sum_{i=1}^{n} (x_i - x_m)(y_i - y_m)}{\sqrt{\sum_{i=1}^{n} (x_i - x_m)^2 \sum_{i=1}^{n} (y_i - y_m)^2}} \tag{2}$$

with $-1 \leq r_{xy} \leq 1$. Herein, x_m and y_m are the sample mean values of *X* and *Y*.

In addition to the value of the correlation coefficient, a second quantity of interest is the *p*-value for testing the null hypothesis of no correlation against the alternative that there is a correlation. The *p*-value provides a measure of the credibility of the null hypothesis, i.e., it is the risk of wrongly rejecting the null hypothesis in view of the observed x_i, y_i. Low values of *p*, e.g., $p < 0.05$, indicate that the correlation between the two quantities *X* and *Y* is significant. For further details on the *p*-value, see [32].

The linear correlation analysis is applied to investigate the correlation between the number of converter power-module failures in a park with the average environmental conditions during the same period. The analysis is carried out on a monthly and, where possible, on a daily scale. A correlation analysis on the daily scale requires knowledge about the exact date on which a converter failure started. By combining the failure data, providing the approximate date of failure and the affected turbine, with the fault messages logged by the SCADA system of the same turbine, it is in the most cases possible to determine the date at which a converter problem started. In case of an existing correlation between the failure and an environmental factor, it can be expected that the conditions being present at the initiation of the problem are those relevant for the failure.

B. Characterization of the Field-Operating Conditions

A simple but important question in the context of failure analysis is if the real operating conditions of the component of interest in the field comply with the specifications this component has been designed for. However, little is known about the real operating conditions of power converters in wind turbines so far.

Due to this, an attempt is made to characterize the operating conditions of the converters in the field. Here, the focus is put on the operating environment inside the converter cabinets. While an estimate of the load profile can be obtained from the 10-min SCADA data, additional data have been collected to investigate the latter aspect: Using battery-driven loggers of the type Lascar EL-USB-2, the temperature and the relative humidity inside the converter cabinets of several wind turbines of type WT1 and WT2 have been recorded over a period of several weeks April–June 2012 with a sampling interval of 30 min. The loggers have been positioned at the upper inside of the converter cabinets.

C. Postoperational Analysis of Converter Modules

In addition to the analysis of failure data and the characterization of the converter operating conditions described previously, several power modules, which had been in operation in turbines of type WT1 at an offshore site, have been investigated. While information about the exact operational age of these power modules is lacking, it can be concluded from the manufacturing dates that their maximum operational age is 6 years.

With the objective to identify the affected parts of the modules and to obtain indications for the mechanisms of failure, the available power modules have been utilized in two different types of analyses:

Nine modules without visible signs of destruction have been subject to different diagnostic measurements using the DSUB connector to the gate-driver board as well as the ac and dc terminals. The tests have covered the measurement of the insulation

TABLE II
CONVERTER-RELATED AVERAGE FAILURE RATES OF WIND TURBINES OF TYPE WT1 AND WT2 AT DIFFERENT SITES

Wind park	Turbine type	Site	Avg. failure event rate [1/turbine/a]	Avg. failure event rate [1/module/a]
Site A	WT1 (DFIG)	Offshore	0.12	0.020
Site B	WT1 (DFIG)	Onshore	0.15	0.025
Site C	WT2 (IG+FPC)	Offshore	0.39	0.021

resistances between different parts of the gate-driver board and the heat sink, of the withstand voltage and of the on-state forward voltage drop of the IGBTs and diodes. In addition, it has included functionality checks of the IGBTs, diodes, and of the module-internal temperature and current sensors.

Two power modules with obvious signs of destruction were subject to forensic analysis. For this purpose, the modules have been opened and inspected visually, by means of an optical microscope and a scanning electron microscope. Additional modules without visible signs of destruction have been subject to more advanced forensic analysis in a specialized test laboratory, including optical and X-ray microscopy inspection, scanning acoustic microscopy (SAM) analysis and scanning electron microscopy/energy dispersive spectroscopy (SEM/EDS). Manual pull tests by means of a small needle tool have been carried out on the bond-wires of power modules with and without visible signs of destruction, with the objective to assess their integrity and attachment to the dies.

In order to ensure that all findings could be related to the field operation of the converter and had not possibly been introduced during the previously described diagnostic measurements, different modules have been used for the two types of analysis.

IV. RESULTS AND DISCUSSION

The presentation and discussion of the analysis results are structured in accordance with the three main analysis tracks introduced in the previous section.

A. Failure-Data Analysis Results

Table II provides a compilation of the average failure-event rates obtained for the different wind parks using (1). Note that, here as well as in the following, a converter failure is considered a single failure event even if several converter modules are affected and might have been replaced sequentially throughout a period of some days.

The failure-event rates calculated for turbines of type WT1 show a good agreement between the offshore Site A and the onshore Site B. In contrary, it is considerably higher for turbines of type WT2 operating at Site C. Interestingly, normalization with the number of converter modules per turbine reveals a very similar average number of failures per module and year, in spite of the different generator-converter topologies of WT1 and WT2 (see Table II).

Additional information available for Site C is the mode of converter failure. The two clearly dominating failure modes are

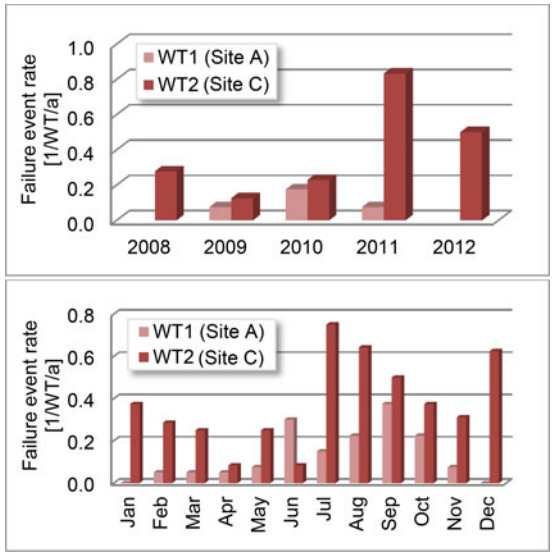

Fig. 3. Temporal distribution of converter failures in turbines of type WT1 (data from Site A, January 2009–April 2011) and WT2 (data from Site C, August 2008–February 2012).

explosion failure and so-called sharing faults, both having approximately equal shares. Sharing faults imply a control-system induced shutdown of the turbine when an unbalanced current-sharing between the paralleled converter units in WT2 is detected. This is usually the case when a converter module fails to switch. It could also have module-external causes like loosened cable connections.

1) Temporal Distribution of Converter Failures: Failure data from WT1/Site A ranging from January 2009 to April 2011 and from WT2/Site C from August 2008 to February 2012 have been used to calculate the average annual failure rates as well as the distribution of failures over the months of the year. These are shown in Fig. 3.

The average annual converter failure rates are found to vary considerably over the years. While the period of observation is too short to identify possible age-related trends in the converter reliability, Fig. 3 reveals that the seasons summer and autumn are most critical with respect to converter failure at the sites considered.

2) Correlation With Climatic Factors and Wind Speed: In order to identify environmental factors being correlated with failure, converter failure data from Site A (WT1) and Site C (WT2) are analyzed in combination with climate data from a nearby measurement station and with wind-speed data recorded by the turbine SCADA systems.

Fig. 4 shows the monthly number of converter failures together with the average values of the ambient temperature, the ambient relative humidity, and the wind speed in the respective month. Not surprisingly, the average temperature is highest during the summer months, while the relative humidity reaches its maxima in the winter and wind speed reaches the highest average values in autumn and winter.

In order to quantitatively assess the correlation between converter failure and the environmental factors temperature, relative

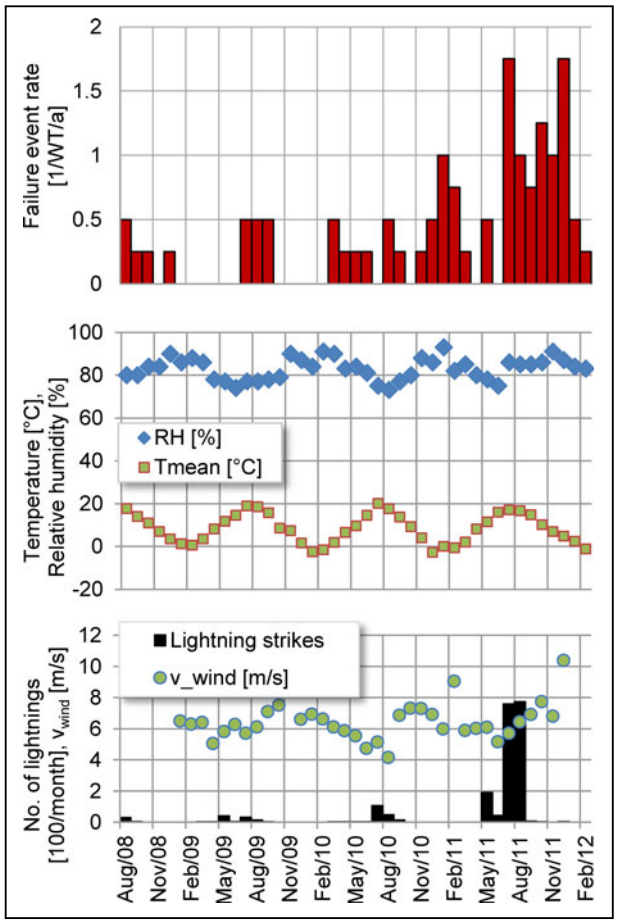

Fig. 4. Converter failures and monthly average values of ambient temperature, relative humidity, wind speed and number of lightning strikes at Site C.

TABLE III
RESULTS OF CORRELATION ANALYSIS; LINEAR CORRELATION COEFFICIENTS OF CONVERTER FAILURE AND ENVIRONMENTAL FACTORS

	Correlation with failure, using		
Environmental factor	monthly avg. data (Site A)	monthly avg. data (Site C)	daily average data (Site C)
Average ambient temperature	$r = 0.46$, $p = 0.014$	$r = 0.14$, $p = 0.36$	$r = 0.04, p = 0.15$ (expl.: $r = 0.03$, $p = 0.34$)
Average relative humidity	$r = -0.33$, $p = 0.082$	$r = 0.28$, $p = 0.07$	$r = 0.04, p = 0.22$ (expl.: $r << 0.01$, $p = 0.98$)
Average wind speed	$r = -0.30$, $p = 0.153$	$r = 0.34$, $p = 0.04$	$r = 0.12, p = 0.0001$ (expl.: $r = -0.005$, $p = 0.86$)
Number of lightnings	n.a.	$r = 0.48$, $p = 0.001$	$r = 0.11, p = 0.0002$ (expl.: $r = 0.15$, $p = 3 \cdot 10^{-7}$)

humidity, wind speed and lightning, linear correlation analysis as described in Section III-A is applied to the data. The resulting correlation coefficients and p-values are compiled in Table III.

Due to a lack of suitable detailed data, the analysis is based on monthly average values and does not include lightning in case of WT1 (Site A). The correlation analysis for WT2 (Site C) is based on both monthly and daily average values. While the first is based on the data shown in Fig. 4, the latter is limited to data from the period January 2009–December 2011 due to data availability. Note that temperature and relative humidity are included as separate factors in Table III, but are not independent from each other, as their instantaneous values are related through the absolute humidity. (At constant absolute humidity and pressure, RH falls with increasing temperature as warmer air can carry a higher amount of moisture.)

In case of WT1 at Site A, the only statistically significant correlation is found between converter failure and ambient temperature. Some negative correlation is observed with the relative humidity. However, as a failure rate decreasing with the relative humidity is physically not plausible, this should mainly be ascribed to the strong negative correlation ($r = -0.82, p < 0.001$) of temperature and relative humidity due to their aforementioned systematic relationship. No statistically significant correlation is found between converter failure and the average wind speed.

In contrast to the WT1-specific results based on data from Site A, no statistically significant correlation is found between converter failure and ambient temperature in the case of WT2 at Site C. While some correlation with the relative humidity is suggested by the monthly average data, the more reliable results obtained from the daily average data disprove this. A stronger, statistically significant correlation is found between the number of failures and the average wind speed. A more detailed analysis based on the daily average wind speed shows that this applies only for the nondestructive failures. In contrast, explosion failure is not correlated with the wind speed.

3) Lightning Impact: In order to further investigate the possible correlation of converter failure with lightning strikes, lightning data from Site C and its surrounding area have been analyzed together with the failure data. On an annual time scale, an extraordinarily high number of lightning strikes in 2011 coincide with a high number of converter failures in that year. In order to quantitatively assess the correlation between converter failure and lightning strikes, linear correlation analysis has been applied to the monthly numbers of converter failure and lightning strikes in vicinity of the wind park. The resulting correlation coefficient of $r = 0.48$ with $p = 0.001$ (see Table III) confirms the visual impression of a strong correlation.

In addition to the analysis on a monthly scale, for the case of Site C, it has been possible to perform a correlation analysis even on the daily scale. As described earlier, this requires exact knowledge of the date on which a failure started. In the present case, the analysis is therefore based on the failure events occurred during January 2009–December 2011, excluding four events reported in the failure data, for which no indication could be found in the SCADA alarm logs.

Interestingly, the much more informative correlation analysis on the daily scale confirms a statistically significant correlation between the number of failures and the number of lightning strikes ($r = 0.11, p = 0.0002$). A particularly significant correlation is found between explosion failures and lightning strikes ($r = 0.15$, $p = 3 \cdot 10^{-7}$). This is a strong indication that lightning strikes are a relevant factor for converter failure and in particular for the failure mode of thermal destruction.

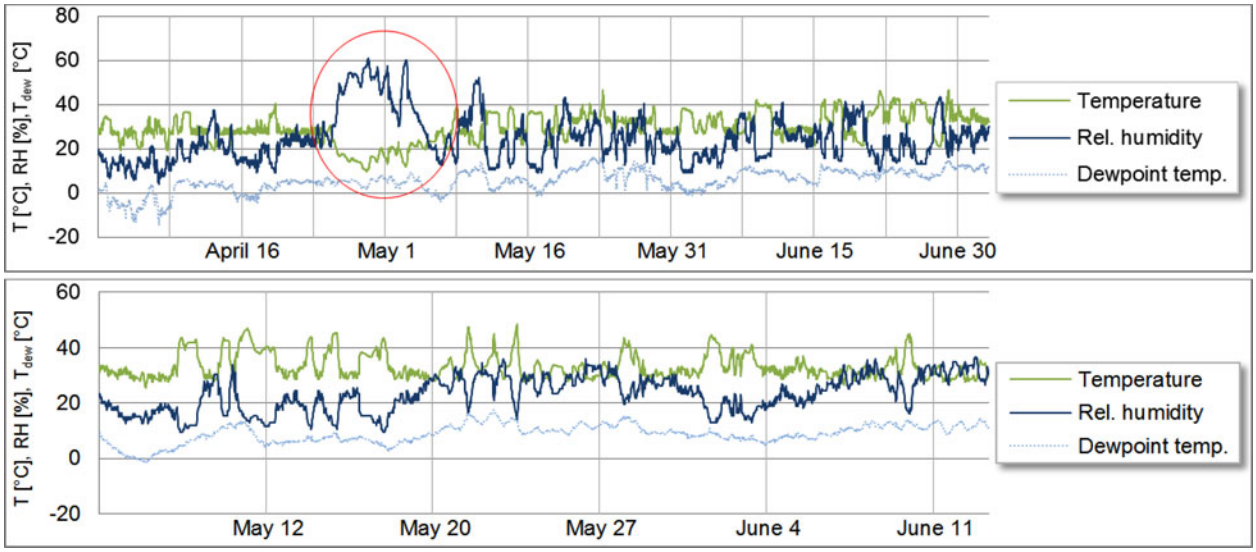

Fig. 5. Temperature, relative humidity, and corresponding dew-point temperature inside the converter cabinet of a turbine of type WT1 (top, data from offshore Site A) and WT2 (bottom, data from offshore Site C).

Among the possible ways in which lightning strikes can have an effect on wind turbines are the direct hit by a lightning strike, radiated electromagnetic interference, a rise in the ground potential or disturbances in the collection grid of the wind park. In addition, periods with frequent converter failure following months with a high number of lightning strikes suggest that lightning might not only lead to immediate failure, but might also cause predamages that lead to failure with some time delay.

B. Converter-Operating Environment in the Field

The operating conditions inside the converter cabinets of turbines of types WT1 and WT2 have been explored by means of temperature and humidity loggers. Fig. 5 shows the conditions measured at a WT1 turbine at Site A and a WT2 at Site C, respectively. During periods of normal (i.e., wind-dependent, intermittent) operation, see, e.g., mid of May to end of June in Fig. 5, the converter-cabinet temperature in WT1 is found to vary around 30 °C, with extreme values reaching approximately 15 °C and approximately 50 °C, respectively, with a relative humidity very rarely exceeding 45%. In case of WT2 at Site C, the converter-cabinet temperature is found to range between 25 and 50 °C, while the relative humidity remains below 40%. Thus, no exceptional conditions are found inside the converter cabinets during normal operation which would be likely to promote converter failure.

An interesting case could be logged on a WT1 turbine at the offshore Site A; see Fig. 5 during end of April and early May: after a standstill period of 9 days and 2 days of major repair work with an opened nacelle, a converter failure occurred during start-up of the turbine on 4 May. Similar cases were reported to have occurred before in the same offshore wind park. The logged temperature and relative-humidity data confirm that this most likely is related to condensation: due to the standstill period, the nacelle cools down and the relative humidity increases to values of approximately 60%. This results in a low difference between the temperature logged at the top inside of the converter cabinet and the corresponding dew-point temperature, which is likely to have caused condensation on the converter modules as these have a high thermal inertia.

In summary, it can be stated that the converter operating conditions are uncritical with respect to temperature and humidity during normal turbine operation but appear to be problematic with respect to condensation after long periods of standstill.

C. Results of the Postoperational Investigation of Converter Modules

Solely power modules from wind-turbines of type WT1 (Site A) have been available for postoperational analysis. Note that all findings presented in this section must therefore be assigned to the WT1 system. Power modules returning from the field for repair included similar numbers of modules from the generator-side converter and from the grid-side converter, indicating that failures occur in both parts of the converter system.

1) Electrical Measurements: Nine converter modules from Site A without obvious signs of damage have been investigated using the tests and measurements described in Section III-C. Among the nine modules are four grid-side and five generator-side modules. While all grid-side modules had been tested before and were known to be defect, the condition of the generator-side modules was unknown. All of them had been replaced in relation with failure of the converter.

Table IV summarizes the results of the measurements. The four grid-side modules were found to have the following defects: 1) nonswitching top IGBTs (one case); 2) nonswitching bottom IGBTs (two cases); and 3) failed current and temperature sensors (one case). Among the generator-side modules, a single failed one has been found, with nonswitching bottom IGBTs. All modules have met the specified withstand voltage of 1200 V.

TABLE IV
RESULTS OF THE ELECTRICAL MEASUREMENTS

Measurement	Comment	Values/results
IGBTs	functionality test top IGBTs	1 not switching, 8 funct.
	funct. test bottom IGBTs	3 not switching, 6 funct.
Diodes	functionality test top diodes	all functional
	funct. test bottom diodes	all functional
Temperature sensor	functionality test	1 defect, 8 functional
Current sensor	functionality test	1 defect, 8 functional
Withstand voltage	measured at 2.35 mA	1275–1375 V
Voltage drop	over the IGBTs	50 A: 0.77–0.80 V; 200 A: 0.93–0.96 V
	over the diodes	50 A: 0.75–0.78 V; 200 A: 0.94–0.97 V
Insulation resistance	between cooling fins+DSUB	7.5–10 MΩ
	between cooling fins and ac, DC+ and DC– terminals	approx. 5–100 kΩ 100–360 GΩ (900 GΩ on 1 very clean module)
	between cooling fins and heat sink	

Because of the fact that all tests and measurements have been performed on complete power modules, it has not been possible to test single-chip functionality. Due to the same reason, it is not possible to distinguish if the nonswitching of IGBTs has been caused by a defect gate-driver board or by failed IGBT chips.

Diodes fail typically in short-circuit mode. In spite of the parallel connection of a large number of diodes inside the modules, it can therefore be concluded from the diode functionality test that all of the diodes have been intact.

The voltage drop and the differential resistances of both the functional IGBTs (R_{CE}) and the diodes, which were determined from the measurements, are found to be in satisfactory agreement with the datasheet values.

Finally, the insulation resistances between the cooling fins of the gate-driver board and the ac terminals, the dc terminals, the outside of the DSUB connector and the heat sink has been measured. An interesting finding is that there is a galvanic coupling between the cooling fins and either an ac or a dc terminal, with a resistance in the range of 5–100 kΩ (see Table IV). A marginal conductance found between the cooling fins and the heat sink can be ascribed to surface contamination of the modules.

2) Forensic Analysis: The disassembly of the power modules obtained for forensic analysis shows that the IGBTs and diodes inside these are covered with an insulating soft potting compound. While the power-electronic devices together with the DCB are protected from the environment by means of the module housing and the above potting compound, the driver board (or printed-circuit board, PCB) is only partially covered: located under the top cover of the power module, it is completely molded by a hard coating on the upper side, while on the downside it is partially accessible for air circulating in the converter cabinet.

The findings obtained during the forensic analysis are summarized in Table V. For the sake of brevity, a detailed description and discussion are limited to a selection of these. Modules M1 and M2, which had been in operation in grid-side converters in WT1, showed signs of severe thermal destruction: in both modules, the center of destruction was located in one of the outer half-bridges. The surrounding plastic case was destroyed by the detonation and large amounts of soot were found inside and on the surface of the module.

In the first investigated power module, denoted M1, evidence was found of high-voltage flashover between a cooling fin soldered to the gate-driver board and a screw fixing one of the half-bridges to the heat sink; see Fig. 6(a) and (b). The dielectric strength of air is approximately 3 kV/mm. Thus, to initiate a flashover over a gap of 7 mm between the cooling fin and the screw, a voltage of approximately 20 kV and therefore a multiple of the normal operating voltage of <1 kV is required. The material transferred from the cooling fin to the screw indicates that the cooling fin must have been on a high negative potential with respect to the screw. Four possible scenarios that might have caused the observed damage were discussed.

1) A lightning strike hitting the surrounding structure found a discharge path through the converter module. The galvanic coupling between the power circuit and the cooling fin revealed by the electric measurements described in the previous section supports this scenario. A possible explanation is that the slip rings connecting the turbine shaft to the structure were not fully functioning.
2) A disturbance in the external grid occurred and the system failed to protect the IGBTs.
3) Static electricity build-up from the rotor blades of the turbine found a discharge path through the module. This phenomenon is known from airplane propellers and helicopters especially if rotor blades are of composite material. The energy involved in that case would be too low to cause the level of damage observed, but it might initiate an arc-flash event. Once an arc-flash event is initiated, a lower voltage level is sufficient to maintain it. A considerable amount of energy with the potential to cause the severe damage observed is typically available in the dc link of wind-turbine converters. However, static electricity build-up from the rotor blades is an unlikely cause of high voltages in the converter as an electricity build-up is usually drained through slip rings on the turbine shaft.
4) A reduction of the air gap by a foreign object could have started an arc flash, which subsequently might have been maintained in the way discussed earlier. A likely foreign object is, e.g., an insect creeping into the open module. Bartram [25] showed that flies are attracted by the silicone gel typically covering the power-electronic devices in wind-turbine converters. In spite of the often large distances from the coast, large numbers of dead insects have been found inside the turbines and even inside the converter cabinets in one of the considered offshore wind parks (Site C), which makes the above a plausible explanation scenario.

In the context of the described flashover damage, the air gap between the cooling fin and the screw is regarded relatively small. Besides using a design with a larger air gap, a measure to prevent flashover in this part of the module could be the introduction of a thin insulating sheet of, e.g., Kapton or Mica in the gap.

TABLE V
RESULTS OF THE FORENSIC ANALYSIS

Analysis method	Module M1	Module M2	Module M3	Module M4
	Partly thermally destructed		No signs of destruction	
Visual inspection, optical microscopy	high-voltage flashover between PCB cooling-fin and screw to heat sink	signs of high current though power-module including displaced bus bars	visible contamination on PCB (see also SEM/EDS analysis next)	remelted solder joints and burned resistor on PCB
	signs of high current in signal contact springs connecting PCB and IGBTs (discolorations)	degraded thermal paste between DCB and heat sink		
	no damage or corrosion of bond wires in undestroyed half-bridges			
	no visible contamination on PCB			
	some fretting on PCB gold contacts (from destruction?)	no fretting on PCB		
	no tin whiskers on PCB			
SEM/EDS	n.a.	fretting spots on bottom of DCB and on adjacent heat-sink surface	salt and corrosion products on PCB creating a conductive path	n.a.
X-ray microscopy	n.a.	n.a.	acceptable solder-joint appearance on PCB	
SAM analysis	n.a.	n.a.	die-attach solder of all chips (IGBTs, diodes) intact	
Limited microsectioning, opt. microscopy inspection	n.a.	n.a.	n.a.	die-attach solder and bond-wire attachment intact
Visual inspection of DCB	n.a.	n.a.	no irregularities in DCB plating except slight color shift on one DCB	no irregularities in DCB plating
Manual pull test on bond wires	n.a.	n.a.	all bond-wires normally bonded to chips and substrate	all tested bond-wires normally bonded to chips and substrate (partial check)

n.a.: not applied.

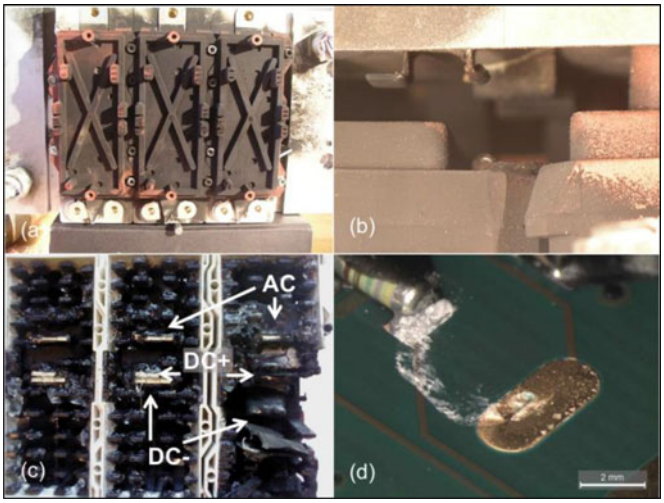

Fig. 6. (a) and (b) Signs of high-voltage flashover between a screw and a PCB cooling fin, (c) melting pattern in module-internal busbars, (d) contamination and corrosion products on a gate-driver board.

Not surprisingly, also the analysis of the second destructed module, M2, has revealed signs of very high currents through the module. As Fig. 6(c) shows, all three paralleled half-bridges have the same damage pattern: The connections to the DC+ and the ac side show melting in the same contact points. The considerable displacement of the DC– connection from the DC+ connection observed in Fig. 6 (c) gives evidence of a very strong energy release. Regarding the origin of this energy release, no clear evidence could be found. Among the potential mechanisms resulting in destruction is a resonance of the signal contact springs connecting PCB and IGBT gates. This might lead to intermittent loss of the contact between the gate-driver board and the IGBTs and therewith cause the so-called floating gate in the IGBT, i.e., a state between ON and OFF. A floating gate in an IGBT results in a strong heat-up and leads finally to thermal destruction.

An irregularity discovered in module M2 was corroded spots at the bottom side of the DCB as well as on the upper side of the nonanodized aluminum heat sink. In the area of these spots, no thermal grease was found left between the two surfaces and the inert gold-layer covering the bottom side of the DCB was damaged. SEM/EDS analysis of one of the spots showed that it predominantly consists of aluminum and copper, i.e., of material from the heat sink and the DCB. No traces of chlorine were found, which could have pointed to the ingress of salt. The positions of the spots coincide with the points in which the DCB is pressed to the heat sink by means of the plastic pins visible in Fig. 6(c). In combination with the chemical composition of the spot, this observation strongly suggests the presence of fretting: Under the impact of mechanical pressure, thermal cycling and possibly also promoted by vibration, abrasive wear of the two surfaces takes place. The craters caused by this effect were found to reach no further than approximately 75 μm over and into the DCB surface, which is not considered critical for the integrity of the DCB. An interesting question requiring further investigation is if the fretting spots are afflicted with an increased thermal resistance, as only in that case, it would be considered a reliability-critical phenomenon. Possible countermeasure concerning the formation of the observed spots could be the anodizing or the creation of a finer structure of the heat-sink surface. An additional observation made in module M2,

but also in several nondestructed modules was a deterioration of the thermal grease between the DCB and the heat sink: this appeared to be relatively dry and seemed to have been applied in relatively small amounts, not completely covering the interface area of the DCB and the heat sink. A deterioration of the thermal grease can cause an increase in the thermal resistance to the heat sink and might in this way lead to overheating or accelerated aging of the power devices.

In addition to the analysis of two severely damaged modules M1 and M2, two grid-side converter modules without any visible signs of destruction, denoted M3 and M4, were investigated (see summary of findings in Table V). The primary objective was to examine if the converter-module malfunctions could be connected to fatigue-related damages in the half-bridges, specifically to crack formation in the die-attach solder of the IGBTs and diodes, or to bond-wire fractures.

The key finding in module M3, which also constitutes a possible failure cause, was the observation of contamination spots and likely corrosion products at several positions on the PCB; see Fig. 6(d). A SEM/EDS analysis of the contamination revealed the presence of sodium and chloride, indicating impact from the sea based environment, i.e., moisture and salt.

The SEM/EDS analysis of the contamination observed between a component pad and a connector pad showed a dominant content of tin, chloride and oxygen, which points to corrosion products. These have formed a possible path for electrical (ionic) conduction during field operation.

Also, in case of module M4, the damage was found to be located on the PCB: optical inspection revealed remelted solder joints in addition to a burned metal electrode leadless face resistor. An X-ray inspection of this area showed that also on the upper, molded side of the driver board, joints were remelted. Additional X-ray inspection of the driver board did not reveal any further damages or discrepancies of PCB components or solder joints.

Fig. 7(a) shows an image from the X-ray inspection of various driver-board solder joints in converter module M3. Apart from a somewhat uneven via-hole plating (in M3 and M4) and some solder spatter and voiding in solder joints of passive components (in M3), the X-ray inspection indicated a generally acceptable solder joint appearance in both M3 and M4.

The bond-wire integrity of all the bond wires in M3 and a part of the bond wires in M4 was manually tested by careful pulling with a thin needle tool. All bond wires tested in this way showed satisfactory bonding to chips and substrate, respectively.

Fig. 7(b) shows an image from SAM analysis of the die-attach solder of the IGBT and diode chips of a half-bridge in converter module M3. The SAM analysis showed similar acoustic signal response from all chips in the half-bridges of both M3 and M4, indicating intact die attach solder in all chips.

Finally, the results of the SAM analysis and the bond-wire pull test have been verified by means of microsectioning and cross-sectional inspection of two IGBT chips. Fig. 7(c) and (d) shows optical microscopy cross-sectional images of an IGBT chip from a half-bridge in converter module M4. The cross-sectional inspections revealed intact die-attach solder without any signs of crack initiation. The bond-wire connections showed

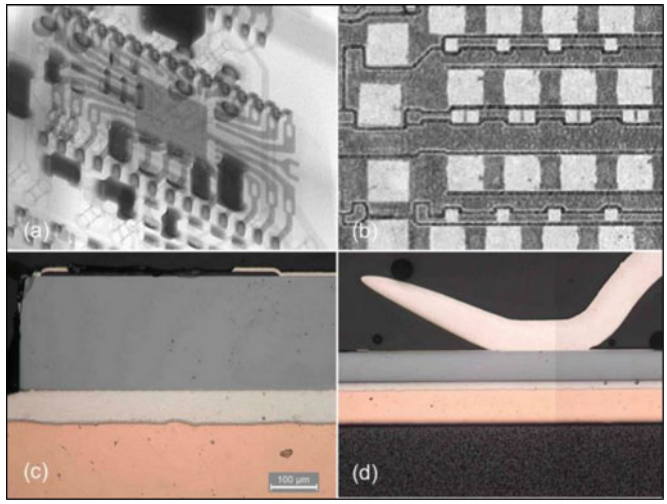

Fig. 7. (a) X-ray inspection of driver-board solder-joints, (b) graphical representation (excerpt) of scanning-acoustic-microscopy signal from die-attach solder of IGBT and diode chips, (c) cross-sectional inspection of die-attach solder, and (d) bond-wire attachment to chip.

largely satisfactory attachment, apart from small crevices at the bond-wire heel. This could be the initial stage of a fatigue crack, but could also have been caused by a not fully melted bond zone during the wire-bonding operation.

In total, the cross-section inspection supports the observations from the manual pull test of the bond wires and the SAM analysis of the die-attach solder, according to which the observed module failure was neither caused by poor solder-joint quality nor by bond-wire damage.

V. Conclusion

This paper has presented a field-experience based root-cause analysis of the frequent failure of power-electronic converters in wind turbines. A multitrack approach has been used and applied to two types of turbines comprising a DFIG with partially rated converter and an induction generator with fully rated converter, respectively. A comprehensive analysis of converter-specific failure data has been carried out. It has included a consideration of temporal patterns in the failure occurrence as well as an investigation of the correlation between failure and different environmental factors, namely the ambient temperature, the ambient relative humidity, the wind speed, and the number of lightning strikes in vicinity of the wind park. Furthermore, the operating environment inside the converter cabinets in the field has been explored on selected turbines by means of temperature and humidity loggers. Converter modules, which had returned from operation in the field, have been investigated by means of electrical measurements and methods of forensic analysis.

The failure-data analysis has not provided any indications that converter failure occurs more frequently offshore than onshore. Similar failure rates per power module have been found in the two turbine types in spite of their different generator-converter topologies. In the turbine with DFIG, both the generator-side and the grid-side converters have been subject to failure, indicating that the severe thermal cycling taking place in the generator-side

converters of DFIG turbines is not among the predominant failure causes. In addition, the postoperational investigation of power modules from DFIG turbines did not reveal any signs of bond-wire damage or solder degradation. These findings suggest that, in contrast to the common perception reflected by the literature on power-converter reliability, the fatigue-related effects of bond-wire damage and solder cracking being the principle failure mechanisms of power electronics in other applications are no predominant cause of failure in the investigated wind turbines. This is in agreement with the statement in [15] that the power cycling lifetime of modern power modules is high enough not to be a lifetime-limiting factor in wind turbines.

Instead, the analysis has revealed indications of insufficient protection of the converter hardware against the environment. Traces of salt and related corrosion leading to unwanted conductive paths were discovered on a power-module driver-board. Insects, which are known to be attracted by soft-potting substances used in power modules, were found inside converter cabinets, where they might reduce insulation-relevant air gaps and cause flashover. The inadequate protection of wind-turbine converters against the environment identified in the present work is in agreement with earlier observations reported in [25], which included the presence of dust and flies in power modules returned from wind turbines.

With respect to temperature and humidity, the conditions inside the electrical cabinets were found uncritical during normal turbine operation but are problematic with respect to condensation after long periods of standstill with disconnection from the grid. In spite of the uncritical converter-cabinet temperatures, deteriorated thermal paste found in several power modules can hinder the heat dissipation from the power devices to the heat sink and in this way cause local overheating and accelerated aging of both driver boards and power devices.

A significant correlation between lightning strikes and converter failure has been observed. This is supported by the results of the forensic analysis, in which a converter module was found with potential signs of electrical overstress. To clarify the causal relationship of nearby lightning strikes and converter damage is an important task for future investigation.

The findings from the present work should be regarded in view of the limited extent of the study: for the two investigated wind-turbine types and their converter systems, the evaluation of the available data basis, which covered approximately 370 years of wind-turbine operation, and the postoperational investigation of 13 power modules could provide indications regarding probable failure mechanisms and causes of the observed converter failures. While this is regarded an important initial step, an extended, directed analysis is considered necessary in order to move from indications to clear evidence and, in the next step, to remedial measures.

This is subject of a new German research cluster, in which a large number of involved companies join forces with academia under the lead of Fraunhofer IWES to deepen the efforts within this area. Besides an extensive root-cause analysis, in which the field-experience based approach presented here is applied in a larger context, and the development of suitable remedial measures, the research topics of the cluster include condition monitoring of electronics and fault-tolerant generator–converter systems, with the overall objective to enhance the reliability and maximize the availability of power converters in wind turbines.

ACKNOWLEDGMENT

The authors would like to thank U. Axelsson, P.-E. Amby Christensen, M. Forsom, L. Højholt, J. Jørgensen, M. K. Pedersen, and T. Söderlund at Vattenfall for valuable discussions and/or technical support to the project. The wind-turbine failure and operating data as well as the converter hardware analyzed in this work were provided by Vattenfall. The climate data were supplied by the Swedish Meteorological and Hydrological Institute and the Danish Meteorological Institute. Parts of the postmortem analysis of converter hardware were carried out at Swerea IVF, Gothenburg.

REFERENCES

[1] M. Wilkinson and B. Hendriks. (2011). "Report on wind turbine reliability profiles—Field data reliability analysis." *RELIAWIND Project Report* [Online]. Available: www.reliawind.eu/files/file-inline/110502_Reliawind_Deliverable_D.1.3ReliabilityProfilesResults.pdf

[2] F. Spinato, P. J. Tavner, G. J. W. van Bussel, and E. Koutoulakos, "Reliability of wind turbine subassemblies," *IET Renewable Power Gener.*, vol. 3, no. 4, pp. 387–401, Dec. 2009.

[3] B. Anjar, M. Dalberg, and M. Uppsäll, "Feasibility study of thermal condition monitoring and condition based maintenance in wind turbines," ELFORSK, Stockholm, Sweden, Tech. Rep. 11:19, 2011.

[4] F. Blaabjerg, M. Liserre, and K. Ma, "Power electronics converters for wind turbine systems," *IEEE Trans. Ind. Appl.*, vol. 48, no. 2, pp. 708–719, Mar. 2012.

[5] C. Busca, R. Teodorescu, F. Blaabjerg, S. Munk-Nielsen, P. Rodriguez, L. Helle, T. Abeyasekera, and M. Sztykiel, "Press pack IGBTs: A reliable solution for medium voltage multi-megawatt wind turbine power converters," presented at the 10th International Workshop on Large-Scale Integration of Wind Power into Power Systems as well as Transmission Networks for Offshore Wind Farms, Aarhus, Denmark, Nov. 25–26, 2011.

[6] A. Birolini, *Reliability Engineering: Theory and Practice*, 7th ed. Heidelberg, Germany: Springer-Verlag, 2014, ch. 1.

[7] M. Ciappa, "Selected failure mechanisms of modern power modules," *J. Microelectron. Rel.*, vol. 42, nos. 4/5, pp. 653–667, 2002.

[8] S. Yang, D. Xiang, A. Bryant, P. Mawby, L. Ran, and P. Tavner, "Condition monitoring for device reliability in power electronic converters: A review," *IEEE Trans. Power Electron.*, vol. 25, no. 11, pp. 2734–2752, Nov. 2010

[9] R. Wu, F. Blaabjerg, H. Wang, M. Liserre, and F. Iannuzzo, "Catastrophic failure and fault-tolerant design of IGBT power electronic converters—An overview," in *Proc. IEEE Ind. Electron. Soc. Annu. Conf.*, Nov. 2013, pp. 505–511.

[10] E. Wolfgang, "Examples for failures in power electronics systems," in *Proc. Tuts. Rel. Power Electron. Syst.*, Apr. 2007, pp. 1–5.

[11] S. Yang, A. T. Bryant, P. A. Mawby, D. Xiang, L. Ran, and P. Tavner, "An industry-based survey of reliability in power electronic converters," *IEEE Trans. Ind. Appl.*, vol. 47, no. 3, pp. 1441–1451, May/Jun. 2011.

[12] C. Busca, R. Teodorescu, F. Blaabjerg, S. Munk-Nielsen, L. Helle, T. Abeyasekera, and P. Rodriguez, "An overview of the reliability prediction related aspects of high power IGBTs in wind power applications," *Microelectron. Rel.*, vol. 51, nos. 9–11, pp. 1903–1907, Sep.–Nov. 2011.

[13] E. E. Kostandyan and K. Ma, "Reliability estimation with uncertainties consideration for high power IGBTs in 2.3MW wind turbine converter system," *Microelectron. Rel.*, vol. 52, nos. 9/10, pp. 2403–2408, Sep. 2012.

[14] M. Musallam and C. M. Johnson, "Impact of different control schemes on the life consumption of power electronic modules for variable speed wind turbines," presented at the 14th European Conference on Power Electronics and Applications, Birmingham, U.K., Aug. 30–Sep. 1, 2011.

[15] M. Ikonen, "Power cycling lifetime estimation of IGBT power modules based on chip temperature modeling," Ph.D. dissertation, Dept. Elect. Eng. Lappeenranta Univ. Technol., Lappeenranta, Finland, 2012.

[16] K. Ma, M. Liserre, F. Blaabjerg, and T. Kerekes, "Thermal loading and lifetime estimation for power device considering mission profiles in wind power converter," *IEEE Trans. Power Electron.*, vol. 30, no. 2, pp. 590–602, Oct. 2014.

[17] M. Bohlländer, "Lastwechseltestbasierte Lebensdaueranalysemethoden für Leistungshalbleiter in Offshore-Windenergieanlagen (Load-cycling

based lifetime analysis methods for semiconductors in offshore wind turbines),” Ph.D. dissertation, Faculty of Elect. Eng. Inform. Technol., TU Chemnitz, Chemnitz, Germany, 2014.
[18] M. Held, P. Jacob, G. Nicoletti, P. Scacco, and M. H. Poech, “Fast power cycling test of IGBT modules in traction application,” in *Proc. Int. Conf. Power Electron. Drive Syst.*, 1997, pp. 425–430.
[19] B. Ji, X. Song, W. Cao, V. Pickert, Y. Hu, J. Makersie, and G. Pierce, “In situ diagnostics and prognostics of solder fatigue in IGBT modules for electric vehicle drives,” *IEEE Trans. Power Electron.*, vol. 29, 2014, doi:10.1109/TPEL.2014.2318991.
[20] D. Hirschmann, D. Tissen, S. Schröder and R. W. De Doncker, “Reliability prediction for inverters in hybrid electrical vehicles,” *IEEE Trans. Power Electron.*, vol. 22, no. 6, pp. 2511–2517, Nov. 2007.
[21] H. A. Mantooth and A. R. Hefner, “Electrothermal simulation of an IGBT PWM inverter,” *IEEE Trans. Power Electron.*, vol. 12, no. 3, pp. 474–484, May 1997.
[22] H. Huang and P. Mawby, “A lifetime estimation technique for voltage source inverters,” *IEEE Trans. Power Electron.*, vol. 28, no. 8, pp. 4113–4119, Jan. 2013.
[23] H. Wang and F. Blaabjerg, “Reliability of capacitors for DC-link applications—An overview,” in *Proc. IEEE Energy Convers. Congr. Expo.*, Sep. 2013, pp. 1866–1873.
[24] M. Bartram, I. von Bloh, and R. W. De Doncker, “Doubly-fed machines in wind-turbine systems: Is this application limiting the lifetime of IGBT frequency-converters?” in *Proc. 35th Annu. IEEE Power Electron. Spec. Conf.*, Aachen, Germany, Jun. 20–25, 2004, pp. 2583–2587.
[25] M. Bartram, “IGBT-Umrichtersysteme für Windkraftanlagen: Analyse der Zyklenbelastung, Modellbildung, Optimierung und Lebensdauervorhersage,” Ph.D. dissertation, Institute for Power Electronics and Electrical Drives (ISEA), RWTH Aachen, Aachen, Germany, 2005.
[26] H. Wang, M. Liserre, F. Blaabjerg, P. de Place Rimmen, J. B. Jacobsen, T. Kvisgaard, and J. Landkildehus, “Transitioning to physics-of-failure as a reliability driver in power electronics,” *IEEE J. Emerging Select. Topics Power Electron.*, vol. 2, no. 1, pp. 97–114, Mar. 2014.
[27] L. Wei, R. J. Kerkman, R. A. Lukaszewski, H. Lu, and Z. Yuan, “Analysis of IGBT power cycling capabilities used in doubly fed induction generator wind power system,” *IEEE Trans. Ind. Appl.*, vol. 47, no. 4, pp. 1794–1801, May 2011.
[28] F. Fuchs and A. Mertens, “Steady state lifetime estimation of the power semiconductors in the rotor side converter of a 2 MW DFIG wind turbine via power cycling capability analysis,” presented at the 14th European Conference on Power Electronics and Applications, Birmingham, U.K., Aug. 30–Sep. 1, 2011.
[29] R. Pittini, S. D’Arco, M. Hernes, and A. Petterteig, “Thermal stress analysis of IGBT modules in VSCs for PMSG in large offshore wind energy conversion systems,” in *Proc. 14th Eur. Conf. Power Electron. Appl.*, Aug. 30–Sep. 1, 2011, pp. 1–10.
[30] S. D’Arco, T. Undeland, M. Bohlländer, and J. Lutz, “A simplified algorithm for predicting power cycling lifetime in direct drive wind power systems,” in *Proc. 9th Int. Multi-Conf. Syst. Signals Devices*, Mar. 20–23, 2012, pp. 1–6.
[31] S. Konrad, “Ein Beitrag zur Auslegung und Integration spannungsgespeister IGBT-Wechselrichter,” Ilmenau, Germany: ISLE, 1997.
[32] D. C. Montgomery and G. C. Runger, *Applied Statistics and Probability for Engineers*, 6th ed. Hoboken, NJ, USA: Wiley, 2014, ch. 9.

Katharina Fischer received the Dipl.-Ing. degree in electrical engineering and the Ph.D. degree in mechanical engineering from University of Hanover, Hannover, Germany, in 2002 and 2008.

She was a Postdoctoral Researcher with the Chalmers University of Technology, Gothenburg, Sweden, until she joined Fraunhofer Institute for Wind Energy and Energy System Technology, Hanover, as a Senior Scientist in 2012. Her research interests include the reliability, condition monitoring and maintenance of wind turbines.

Thomas Stalin received the M.Sc. degree in mechanical engineering from Mälardalens högskola, Västerås, Sweden, in 1986, and in economics from Uppsala universitet, Uppsala, Sweden, in 1998.

After positions at Enron Wind and Sweden Offshore Wind, he joined Vattenfall Wind Power, Stockholm, Sweden, in 2005, where he currently holds the position of a Senior Wind Technology Expert. His main interest is in the operation and maintenance of wind turbines, with a particular focus on gearbox and converter reliability.

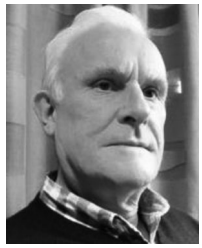

Hans Ramberg received the M.Sc. degree in electrical engineering from the Chalmers University of Technology, Gothenburg, Sweden, in 1977.

He has gathered more than 25 years of experience in testing and validation at Volvo Car Corporation, Gothenburg. His main competences are in the area of environmental effects on electronics in the harsh automotive environment, in corresponding validation and test methods, as well as in cooling of electronics and reliability issues related to temperature stress.

Jan Wenske received the Dipl.-Ing. degree in mechanical engineering and the Ph.D. degree in electrical engineering from the Technical University of Clausthal, Clausthal-Zellerfeld, Germany, in 1994 and 2000, respectively.

For several years, he held different positions in the industry. Since 2011, he has been the Head of the Wind Turbine- and System-Technology Department and the Deputy Director of Fraunhofer Institute for Wind Energy and Energy System Technology, Bremerhaven. Since 2013, he has been a Professor for wind turbine technology at University of Bremen, Bremen, Germany.

Göran Wetter received the M.Sc. degree in mechanical engineering from the Chalmers University of Technology, Gothenburg, Sweden, in 1985.

He has worked in the field of electronics materials analysis for more than 20 years, and is currently a Senior Materials and Failure Analysis Specialist at the Research Institute Swerea IVF, Gothenburg, where he is responsible for the materials- and failure analysis activities regarding electronic products.

Robert Karlsson received the B.Sc. degree in electrical engineering from the Chalmers University of Technology, Gothenburg, Sweden, in 1983.

He was a Research Assistant with the Chalmers University of Technology, in 1983, and since 1987, he has been a Research Engineer. His main interest is the design of power electronics for a large variety of applications.

Torbjörn Thiringer (M’96–SM’10) received the M.Sc. and Ph.D. degrees from the Chalmers University of Technology, Gothenburg, Sweden, in 1989 and 1996, respectively.

He is currently a Professor of applied power electronics at the Chalmers University of Technology. His research interests include the modeling, control, and grid integration of wind energy converters into power grids as well as power electronics and drives for other types of applications, such as electrified vehicles, buildings, and industrial applications.